LONGITUDINAL SPACE CHARGE VIA MULTI-PARTICLE SIMULATION

J.R.Maidment
Rutherford Appleton Laboratory,
Chilton, Didcot, England

E.A.Karantzoulis
Deutsches Elektronen-Synchrotron DESY,
Notkestrasse 85, D-2000 Hamburg 52, West Germany

Summary

Some features of a longitudinal simulation code, PHAEDRA, written for use on the IBM mainframes at RAL and DESY are described. The code may be viewed as one-dimensional in that no account is taken of transverse motion. The numerical methods chosen to evaluate longitudinal space charge forces are discussed. Code predictions are compared for some analytic cases. The results obtained in simulation of DESY III [1] are presented and discussed.

Introduction

During design studies for the proton rf systems of both the injector synchrotrons and main ring of HERA [2] a number of unconventional proposals for rf gymnastics were evaluated using a series of "one-off" tracking codes. Features of these, such as programmed rapid changes of voltage and phase, have been incorporated into PHAEDRA, however, as the final schemes for acceleration and transfer do not rely on such manipulations, we concentrate here on broader aspects of the numerical methods. In particular we assess the extent to which one can believe the predictions, comparing results for cases which may be solved analytically.

Space charge plays a significant role in determining the dynamics close to the injection energy (50MeV) in DESY III, the slow cycling, 7.5GeV/c booster for HERA and assumptions allowing analytic estimates of expected behaviour [3] have been made when specifying system design parameters We therefore used the code to investigate the validity of those studies.

Difference Equations

We assume there is only one accelerating cavity in the ring, or that we may represent all the cavities by the total voltage applied at a single azimuth and write the equations describing the longitudinal motion of a particle with respect to that of a synchronous particle as:

$$\Delta\gamma_{n+1} = \frac{eV}{m_0c^2}(\sin\phi_n - \sin\phi_{s,n}) + \frac{\gamma_n}{\gamma_{n+1}}\left(\frac{\gamma_{n+1}^2 - 1}{\gamma_n^2 - 1}\right)^{1/2}\Delta\gamma_n + \frac{eV_{sc}(\phi_n)}{m_0c^2}$$

$$\Delta\phi_{n+1} = \Delta\phi_n + 2\pi h\eta\left(\frac{\gamma_{n+1}}{\gamma_{n+1}^2 - 1}\right)\Delta\gamma_{n+1}$$

where the subscripts n,n+1 refer to successive revolutions, $\Delta\gamma = \gamma - \gamma_s$ and $\Delta\phi = \phi - \phi_s$.

For a line charge distribution the total voltage per turn experienced by a particle, including that contribution due to the (inductive) chamber impedance, may be expressed as:

$$V_{sc}(\phi) = -eh^2\frac{\beta c}{R}\left(\omega L - \frac{g_0 Z_0}{2\beta\gamma^2}\right)\frac{d\lambda(\phi)}{d\phi}$$

Where ω = angular revolution frequency, L = effective wall inductance, Z_0 = 377 ohms, g_0 is a geometric factor [4] and $\int_{\phi}^{\phi+2\pi}\lambda(\phi)d\phi = N$, the no of particles per bunch. The line density is evaluated once per turn thus implicitly assuming that the distribution changes only slowly within the revolution time.

Space Charge Algorithms

The chief problem in numerically evaluating the line density $\lambda(\phi)$ and its derivative is to reduce the statistical noise due to the (relatively) small number of macro-particles whilst retaining real high frequency density modulation. To this end we have examined the behaviour of two techniques, firstly a digital filter (DF)and secondly a method using Fourier transforms (FT) coupled with selective attenuation of high frequency components. In both cases an array of discrete values of line density is formed using a binning technique which employs linear assignment of macro-particle charge to neighbouring bins. This in itself gives a degree of pre-smoothing when compared with simple nearest bin assignment.

The choice of number of bins coupled with the number of macro-particles used determines not only the degree of noise but also the cpu time needed per mapping and the ranges quoted below reflect the influence of the mainframe batch processors upon which the code has been run. We ran test cases with at most 10,000 macro-particles and up to ~250 bins covering 2π radians of rf phase.

The DF technique places a specified number of bins over that phase length which just encloses the particles and the resultant line density is smoothed by adjusting each value based on a quadratic fit over 3 neighbouring, but not necessarily adjacent, bins. The differential is produced by differencing these smoothed values and then applying a further averaging via a quadratic fit. The number of bins and the range of the local fit were optimised by generating a number of analytic line density functions, including random noise, and comparing the smoothed derivative with the analytic values.

For the FT method we use a fixed no. of bins spanning 2π in rf phase, form the transform of the discrete array and attenuate the resulting components using a "low pass filter" with gaussian roll-off. The derivative is formed by the standard complex multiplication followed by forming the inverse transform. The free parameters are the no. of unattenuated components and the width of the roll-off. These were optimised as described for the DF method above and it was possible to provide a function describing this optimum in terms of the second and fourth moments of the binned distribution.

The array of derivative values resulting from either method is passed through a common block to the mapping routine where it is scaled by the energy dependent terms and the energy change appropriate for a particle at a given ϕ coordinate is found by linearly interpolating between adjacent values. This does not involve further calculation over the macro-particle array since the needed information has already been calculated in the original line density routine.

Both the DF and FT space charge solvers have been incorporated into the code. The user may choose, via input data, whichever he wishes. Bin number defaults are 32 for DF and 128 for FT coupled with 10,000 particles. These values influence the highest frequency of bunch shape modulation which can be resolved and may not necessarily be appropriate for all cases. In addition, if the FT solver is chosen, the user may overwrite the recommended "low-pass filter" smoothing parameters if so desired.

Analytic Comparison

Empirical adjustments to obtain fits to arbitrary (known) derivative functions alone are not a sufficient test of the extent to which we can believe tracking predictions. We therefore compared in some depth the code predictions when applied to a phase space distribution for which matched conditions may be analytically calculated and under which the distribution is stationary. Such a distribution is that with elliptic energy density as discussed by Hofmann and Pederson. [5]

The phase space density of the H-P distribution is given as a function of the Hamiltonian, by

$$g(\Delta\gamma,\phi) = g(H) = k(H_b - H)^{1/2}$$

where H_b is the Hamiltonian of the bunch boundary. The energy density is elliptic and the line density has the same shape as the potential, in this case cosine-like. An input data H-P generator was coded together with a general analysis routine which finds the parameters of the matched H-P distribution given the bunch area and then processes the given set of tracked coordinates to produce the cumulative phase space density for prescribed fractions of the total number of particles used. The deviation of this cumulative density from the theoretical function together with that fraction for which $H > H_b$ are used as measures of the tracking accuracy. The statistically allowed variation of the density measure was estimated by using the generator to produce 500 initial distributions and then process them with the analyser.

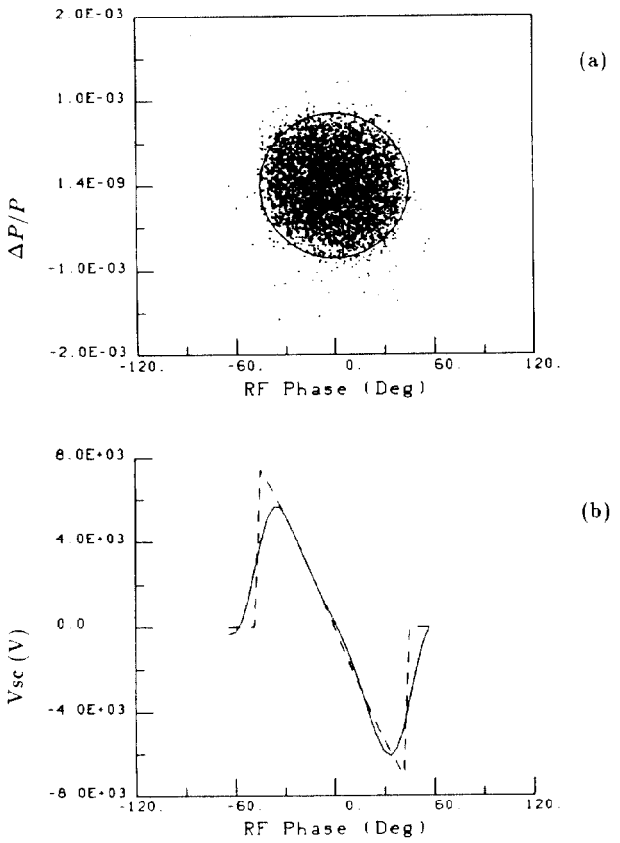

Fig 1. (a) Phase space plot. (b) Space charge voltage array (solid line) of a long term tracked H-P distribution. The dashed line is the theoretical space charge voltage of the initial distribution

Several distributions, varying in phase extent from $\pm 3\pi/4$ to $\pm\pi/4$, with $0° \leq \phi_s \leq 25°$ and with $0.2 \leq V_{sc}/V_{rf} \leq 0.5$ were tracked. For $\phi_s = 0°$ the analytic value of V_{sc} was calculated and used to overwrite the discrete array and thus check that the error arising from linear interpolation was insignificant. Most were run for 2000 revolutions corresponding to between 5 and 25 synchrotron periods. A few selected runs were performed with up to 100,000 revolutions.

Figure 1. shows the phase space plot and calculated space charge voltage for an input distribution of phase extent $\pm\pi/4$ and $\phi_s = 0°$ after tracking for ~80,000 turns via the DF method. Figure 2. shows the resultant cumulative density. The case shown corresponds to ~900 synchrotron periods after which time some 4% of the 5000 particles lie outside the input phase space area. This long term behaviour is typical of both FT and DF algorithms, in the shorter term (~100 synchrotron periods) the cumulative density is statistically stationary and ≤~1% have $H > H_b$.

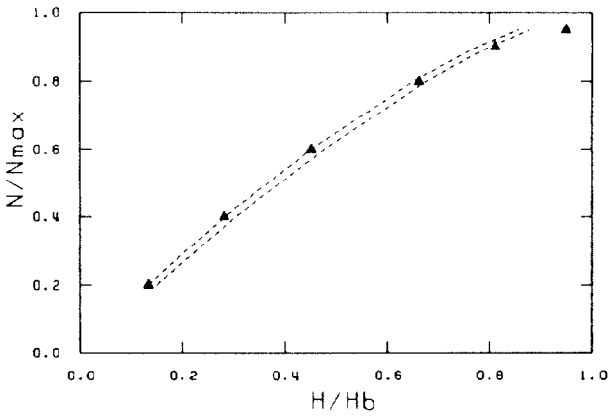

Fig 2. Cumulative density compared with theory for the distribution of Fig 1.

Simulation in DESY III

The early stage of acceleration in DESY III consists of three distinct steps. Firstly quasi-adiabatic trapping of the 50MeV injected linac beam within 10ms during which time the rf voltage is raised from 0.5 to 18kV following an iso-adiabatic law such that α_c, the adiabaticity parameter [6], is ~0.1. Secondly the main bending field is raised as a quadratic function of time until after a further 100ms the maximum rate of field rise, equivalent to dp/dt~5GeV/c/s, is reached. Finally the field increases linearly with time maintaining the acceleration rate constant.

As input distribution we used 5000 particles, uniformly distributed in phase $(-\pi,\pi)$ and gaussian in energy deviation with rms ~59keV but cut off at 2σ. The area of the enclosing rectangle in phase space is 0.072eVs, the nominal linac specification. The previous analytic estimates [3] showed that an rf voltage ≥ 16.5kV is needed to ensure that the minimum bucket area, which occurs at the time of maximum dB/dt, contains this injected emittance.

After each application of the mapping, the particles were scanned and those with phases outside the sampled 2π region were replaced appropriately within the region. This simulates the neighbouring bunches and is only significant during the trapping process. To simulate the transverse momentum acceptance those particles with momentum deviation $\geq \pm 1.5\times10^{-2}$ were removed.

Figure 3. shows phase space scatter plots, plus the corresponding space charge voltage arrays produced by the FT method at; (a) the end of trapping. (b) the end of quadratic field rise and (c) after

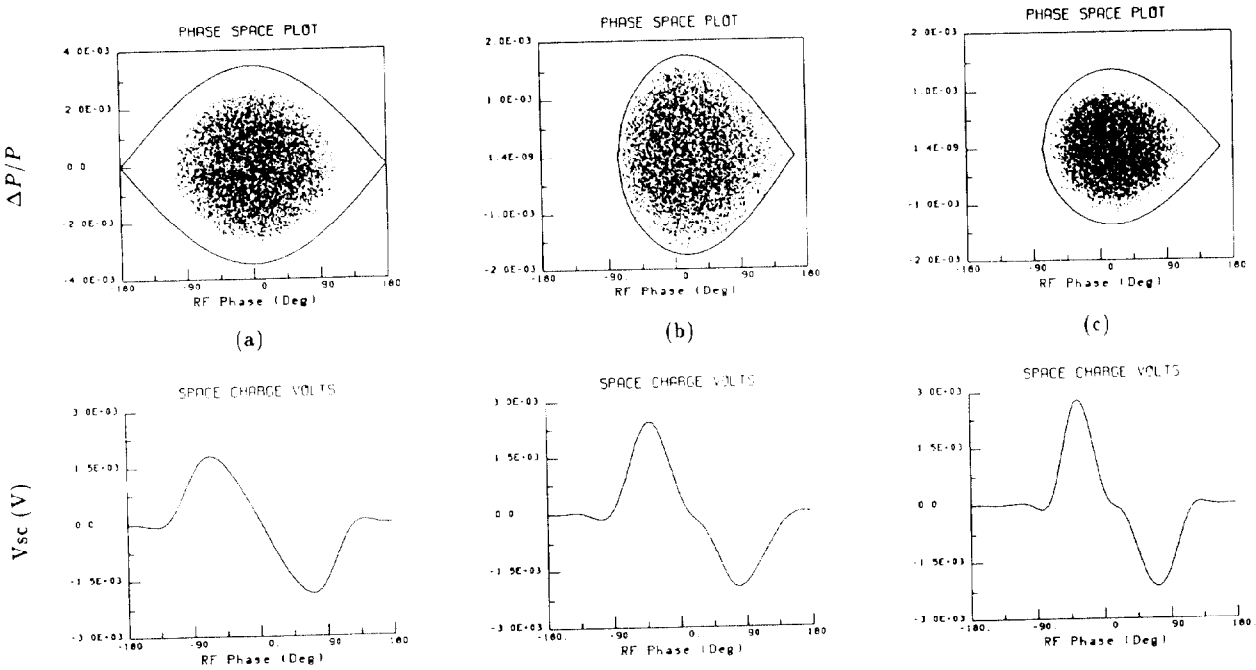

Fig 3. Phase space plots and space charge voltages during simulation in DESY III ,
(a) after trapping (b) 100 ms later (c) after a further 100 ms

a further 100ms of linear field rise. Particle loss, of $<1\%$, occurred within ± 30ms of the start of constant dB/dt. A total of $\sim$100,000 mappings were used in this simulation of 210ms real time and required $\sim$160 mins of cpu time on the IBM 3084Q at DESY. At RAL, where an IBM 3090-200E is available, the cpu required was some 50mins which is accounted for by the faster processor cycle time. The same simulation was run using the DF algorithm, giving very similar results but using $\sim 10\%$ less cpu time.

Analysis of the tracked distributions with respect to matched H-P bunches of the initial input phase area, using the density measure outlined above, shows that the resultant bunches have a denser core and that some particles form a halo beyond the expected phase space limits. The density profile is consistent with the gaussian energy distribution used as input data and the halo increases from ~ 0.5 - 1% over the time scale of Figure 3.

Conclusions

We have demonstrated, by using the analytic values for the array of space charge voltages, that the difference equations represent well the motion of one class of stationary distribution. Both numerical space charge algorithms described display similar non-perfect behaviour. Increasing the number of macro-particles and/or subdividing the turn to evaluate $\lambda(\phi)$ at some average azimuth may improve the accuracy but at the expense of greater computing overheads. The simulation for DESY III does not invalidate the earlier analytic studies.

Acknowledgements

We are grateful to C.W.Planner and C.R.Prior for many useful discussions and to the latter for kindly making available a number of FORTRAN random function generators.

References

1 G.Hemmie, J.R.Maidment, "DESY III, The new proton injector for HERA", Proceedings of the US National Accelerator Conf., Washington, 1987.

2 G.A.Voss, "The HERA Project", These Proceedings.

3 E.A.Karantzoulis, J.R.Maidment, "Beam dynamics at low energy in DESY III", DESY HERA 86-01, 1986

4 A.Hofmann, "Theoretical aspects of the behaviour of beams..", CERN 77-13, pp 139-174, 1977

5 A.Hofmann, F.Pederson, "Bunches with local elliptic energy distributions", IEEE Trans. Nucl. Sci., NS-26, pp 3526-3528, 1979 .

6 D.Boussard, "CAS, Antiprotons for colliding beam facilities", CERN 84-15, pp 261-290, 1984